Issues with increasing bioethanol productivity: A model directed study

Hyun-Seob Song and Doraiswami Ramkrishna†

School of Chemical Engineering, Purdue University, West Lafayette, IN 47907
(*Received 3 September 2009 • accepted 31 October 2009*)

Abstract−We explore a way to improve the efficiency of fermentation of lignocellulosic sugars (i.e., glucose and xylose) to bioethanol in a bioreactor. For this purpose, we employ the hybrid cybernetic model developed by Song et al. (Biotechnol and Bioeng, **103**: 984-1000, 2009), which provides an accurate description on metabolism of recombinant *S. cerevisiae* due to its unique feature of accounting for cellular regulation. A comprehensive analysis of the model reveals many interesting features of the process whose balance is critical for increasing the productivity of bioethanol. In particular, the addition of extra xylose to the medium may increase ethanol productivity (a somewhat counterintuitive result as xylose metabolism is slower!), but one that must be orchestrated with control of other important variables. Effects of xylose addition are shown to be different for different reactor environments. In a batch culture, xylose addition substantially improves ethanol productivity at low sugar concentration (e.g., about 45% up by increasing initial xylose concentration from 10 to 30 g/L with glucose concentration of 20 g/L), but worsens it at high sugar concentration (e.g., about 10% drop by increasing xylose concentration from 40 to 160 g/L with glucose concentration of 80 g/L). On the other hand, the productivity of chemostats is constantly improved by increasing the ratio of xylose to glucose level in the feed. It is found that multiple local maxima can exist in chemostats and, consequently, optimal composition for mixed sugars is different depending on the allowable range of xylose addition. Batch operation, however, is found to be superior when mixed sugars are consumed slowly, while continuous operation becomes attractive for rapidly metabolized sugars such as pure glucose. Optimal reactor configurations for given lignocellulosic sugars are shown to depend on calculated operating curves. Reasonably close comparison of model simulations with existing batch fermentation data provides support in part to the value of the current effort. The lesson that emerges is the importance of modeling in improving the efficiency of bioprocesses.

Key words: Bioethanol Productivity, Hybrid Cybernetic Model, Optimization, Sugar Composition, Recombinant *S. cerevisiae*

INTRODUCTION

Concerns about climate change, high oil price, and peak oil have revived worldwide interest in renewable energy to supplement fossil fuels. The forecast of 50% increase in the world energy consumption over the next two decades [1] with its doubling between 2000 and 2050 [2] has greatly enhanced the need for diversifying energy sources. Among various renewable energy technologies currently available, particular attention has been paid to converting biomass to bioethanol (and biodiesel) for use in the transportation sector which accounts for more than two-thirds of the total liquid fuel consumption [1].

The production of bioethanol from plant biomass is not a new concept, as it has been available on a large scale since the first energy crisis in 1973 using crops such as sugar cane, sugar beet, corn and cereals [3]. Unfortunately, the significant use of such crop-derived biofuels creates the so-called 'food-or-fuel debate' due to the competition with food for the feedstock and agricultural lands. This dilemma could be remedied by utilizing lignocelluosic biomass such as forestry (wood, grasses), agricultural (corn stalks, wheat straw,

sugar cane bagasse), industrial (waste from pulp and paper industry), and urban residues (municipal solid waste).

Lignocellulose is a complex substrate, consisting of three major components: cellulose (33-51%), hemicelluose (19-34%) and lignin (20-30%) [4,5]. Cellulose is a homopolymer of glucose, while hemicellose is a heteropolymer composed of hexose (glucose, mannose, and galactose) and pentose sugars (xylose and arabinose). Lignin does not contain carbon sources but provides rigidity to the structure. In a typical composition of common lignocelluosic biomass, glucose (30-40%) and xylose (10-20%) are the most predominant sugars, while the relative portion of the (hemicellose) constituents varies depending on the plant source [4,6]. Lignocellulosic feedstock is first converted to sugars through pretreatment and hydrolysis, followed by fermentation finally to ethanol. Traditionally, *Saccharomyces cerevisiae* has been used for sugar- and starch-based ethanol production, but the same strain is not suitable for converting lignocellulosic sugars since it only ferments glucose (the most dominant), but cannot xylose (the next abundant). Thus, considerable efforts have been made to endow *S. cerevisiae* with the ability to utilize xylose as well as glucose through metabolic engineering [7]. The overall diagram of so-called B2B (biomass to biofuel) process is illustrated in Fig. 1.

Cost-benefit analysis of the ethanolic fermentation process reveals that the processing cost is more dominant (two-thirds of the total cost) than the feed cost [8,9]. It is thus considered important to increase the processing efficiency, not just the sugar conversion alone.

†To whom correspondence should be addressed.
E-mail: ramkrish@ecn.purdue.edu
‡This paper is dedicated to Professor Jae Chun Hyun for celebrating his retirement from Department of Chemical and Biological Engineering of Korea University.
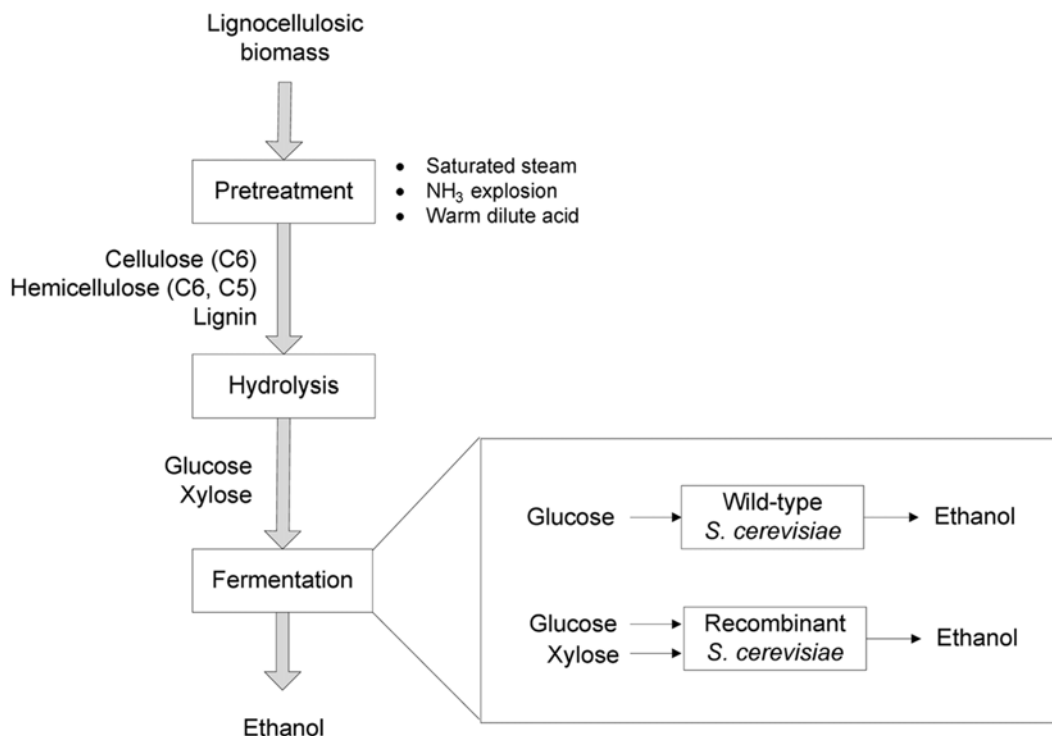
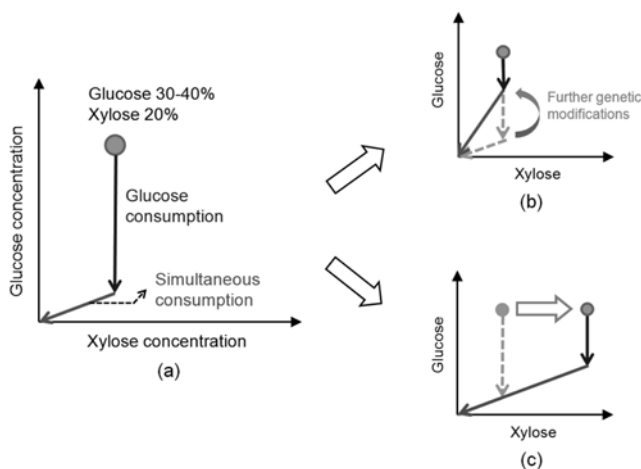Fig. 1. Overall diagram of B2B (biomass to biofuel) processes.

Fig. 2. Schematic representation of (a) current status of fermentation of glucose and xylose by existing recombinant yeast, and strategies for improving ethanol productivity, (b) at the genetic level, and (c) at the reactor level.

In this regard, increasing the *productivity* can be a more important target in bioethanol production than increasing the *yield*. In most cases, the production of bioethanol from cellulosic sugars using recombinant yeast is inefficient in the sense that glucose and xylose are consumed in a sequential manner. As Fig. 2(a) shows, xylose is on standby without being consumed until glucose is depleted to a lower level (say, one tenth or one fifth of xylose level) as denoted by the vertical line, following which simultaneous consumption take places along the tilted line. Obviously, the productivity can be increased if simultaneous consumption occurs earlier when glucose

is present at concentration levels that provide a suitably high growth rate on the mixture. To achieve this, two different strategies can be considered. First, we may develop a more efficient fermenting *organism* through further pathway modifications of existing recombinant yeast. The goal of this attempt at the genetic level corresponds to making the slope of the tilted line steeper (Fig. 2(b)). Alternatively, we may design a more efficient fermentation *process* through optimization of operating conditions or new reactor configuration. For example, if we change initial sugar composition in batch culture by increasing relative portion of xylose in the mixture, this also leads to earlier start of the simultaneous consumption (Fig. 2(c)).

Towards developing the second approach, we investigate optimal ratios of glucose and xylose in batch and continuous cultures to maximize bioethanol productivity. We consider adjusting sugar composition by adding extra xylose to the medium. Xylose is readily obtained as an unconverted sugar from fermentation systems using *wild-type* yeast which converts glucose only. *In silico* analysis is carried out using the cybernetic model constructed by Song et al. [10] which was fully validated using experimental data available in the literature. The cybernetic modeling approach describes cellular metabolism from the viewpoint that a microorganism is an optimal strategist making frugal use of limited internal resources to maximize its survival [11]. Metabolic regulation on enzyme synthesis and their activities is made as the outcome of such optimal allocation of resources. This unique feature of accounting for metabolic regulation endows cybernetic models with the capability to accurately predict peculiar metabolic behaviors such as consumption of multiple substrates in various reactor configurations.

In the following, we briefly present the structure of the model employed in this study. Optimization problems are then formulated for batch and continuous fermenters, respectively. Effects of xylose

addition in both systems are analyzed using model simulations. Based on the results obtained, we present optimal operating conditions for maximizing ethanol productivity, and finally compare the performance of batch and continuous systems.

REACTOR MODEL

For the optimization study, we employ the dynamic metabolic model of Song et al. [10] designed for genetically modified *S. cerevisiae* 1400 (pLNH33) which consumes both glucose and xylose. The recombinant strain was constructed by Ho and coworkers [12] by transforming the plasmids with xylose-converting genes into the host strain *Saccharomyces* yeast 1400. The plasmids contain two exogenous genes encoding xylose reductase and xylitol dehydrogenase which convert xylose to xylitol, and xylitol to xylulose, respectively, and one endogenous gene encoding xylulokinase which converts xylulose to xylulose-5-phophaste.

The model of Song et al. [10] was developed based on the hybrid cybernetic modeling (HCM) idea first proposed by Kim et al. [13]. The HCM is based on the pseudo-steady-state approximation, as it accounts for the dynamics for uptake fluxes using the cybernetic modeling framework, and estimates the intracellular and secretion fluxes from the stoichiometric coupling ratios obtained from the elementary mode (EM) analysis. EMs are a set of sub-networks or pathways composed of a minimal set of reactions necessary to maintain their metabolic functions in steady state [14,15]. All feasible metabolic fluxes are completely described by convex (or non-negative) combinations of EMs. The HCM views metabolism through EMs of the network as representing the major options of the organism to respond optimally to its environment. Uptake fluxes are distributed among EMs in such a way that a metabolic objective (e.g., maximization of growth rate or carbon uptake rate) is accomplished by distributing resources required for selective enzyme synthesis.

To avoid over-parameterization, which may occur in handling a large-scale metabolic network, the HCM for the recombinant yeast strain considered here was constructed based on the minimal subset of EMs which can be selected in a rational way using the metabolic yield analysis developed by Song and Ramkrishna [16]. The resulting model was fully validated using four different sets of experimental data collected by Krishnan et al. [12], which include fermentation data on glucose, xylose, and their mixtures with two different sugar compositions, respectively [10]. The developed model has been used by Wong et al. [17] as a useful tool for studying a model predictive controller with respect to its performance of rejecting abrupt change of feed conditions in continuous fermentation systems producing lignocellulosic ethanol. A set of model equations are now presented below with brief explanations. For more detailed information, one can refer to the original article [10].

Dynamic mass balances for extracellular metabolites can be given in a general form as follows:

$$\frac{d\mathbf{x}}{dt} = \mathbf{S}_x \mathbf{r}_c - D(\mathbf{x} - \mathbf{x}_{IN}) \tag{1}$$

where **x** is the vector of n_x extracellular components, $\mathbf{S}_x$ is the ($n_x \times n_r$) stoichiometric matrix, and **r** is the vector of n_r intracellular and exchange fluxes. The second term of the right hand side of Eq. (1)

is included for the simulation of chemostats where D is the dilution rate, and $\mathbf{x}_{IN}$ is the vector of n_x inlet concentrations of extracellular metabolites. The balance for the biomass c is not shown here by treating it as one of the components of **x**. Under the pseudo-steady-state approximation for intracellular metabolites, the flux vector of metabolic network can be represented by convex combinations of EMs:

$$\mathbf{r} = \mathbf{Z}\mathbf{r}_M \tag{2}$$

where **Z** is the ($n_r \times n_z$) EM matrix, and $\mathbf{r}_M$ is the vector of n_z nonnegative weights to EMs. Without loss of generality, **Z** is assumed to be normalized with respect to a reference substrate so that $\mathbf{r}_M$ implies uptake fluxes through EMs.

In HCMs, fluxes through EMs are described as being controlled by independent enzymes, i.e., for the *j* th mode,

$$r_{M,j} = v_{M,j} e_{M,j}^{rel} r_{M,j}^{kin} \tag{3}$$

where $v_{M,j}$ is the cybernetic variable controlling enzyme activity, $r_{M,j}^{kin}$ is the kinetic term, $e_{M,j}^{rel}$ is the enzyme level relative to their maximum value ($e_{M,j}^{max}$), i.e.,

$$e_{M,j}^{rel} \equiv \frac{e_{M,j}}{e_{M,j}^{max}} \tag{4}$$

Enzyme level $e_{M,j}$ is governed by the following dynamic equation:

$$\frac{de_{M,j}}{dt} = \alpha_{M,j} + u_{M,j} r_{ME,j}^{kin} - (\beta_{M,j} + \mu) e_{M,j} \tag{5}$$

where the four terms of the right hand side represent constitutive and inducible synthesis rates, degradation rate, and dilution rate by growth, respectively, $u_{M,j}$ is the cybernetic variable regulating the induction of enzyme synthesis, and $r_{ME,j}^{kin}$ is the kinetic part of inducible enzyme synthesis rate.

Song et al. [10] classified the full set of EMs consisting in 201 EMs into three groups: glucose- (33 EMs), xylose- (57 EMs) and mixture-consuming (111 EMs) groups. Then, using the model reduction technique of Song and Ramkrishna [16], EMs of each group was reduced to 3, 4, and 5 EMs, respectively. The kinetics for substrate uptakes and enzyme synthesis associated with each group of EMs are given as follows:

$$r_{M,j}^{kin} = \begin{cases} k_j^{max} r_{GLC}^{kin} \ (j=1-3) \\ k_j^{max} r_{XYL}^{kin} \ (j=4-7) \\ k_j^{max} r_{MIX}^{kin} \ (j=8-12) \end{cases}, \quad r_{ME,j}^{kin} = \begin{cases} k_{E,j} r_{GLC}^{kin} \ (j=1-3) \\ k_{E,j} r_{XYL}^{kin} \ (j=4-7) \\ k_{E,j} r_{MIX}^{kin} \ (j=8-12) \end{cases} \tag{6}$$

where k_j^{max} denotes $k_j e_{M,j}^{max}$, and

$$r_{GLC}^{kin} = \frac{x_{GLC}}{K_G + x_{GLC}} \frac{1}{1 + x_{ETH}/K_{I,G}}$$

$$r_{XYL}^{kin} = \frac{x_{XYL}}{K_X + x_{XYL}} \frac{1}{1 + x_{ETH}/K_{I,X}} \tag{7}$$

$$r_{MIX}^{kin} = r_{GLC}^{kin} r_{XYL}^{kin}$$

From Eq. (5) with Eq. (7), the maximum enzyme level at steady state ($e_{M,j}^{max}$) is given as follows:

$$e_{M,j}^{max} = \frac{\alpha_{M,j} + k_{E,j}}{(\beta_{M,j} + \mu_j^{max})} \tag{8}$$

Table 1. Parameter values used in model simulations

EM group	G				X			M				
Index j for EM	1	2	3	4	5	6	7	8	9	10	11	12
$e_i^{rel,0}$ [-]		0.091 $(=e_G^{rel,0})$				0.51 $(=e_X^{rel,0})$		0.43	0.43	0.48	0.21	0.096
$f_{c,j}$ [C-mol/mol]		6				5		26	26	60.4	7.88	6.06
k_j^{max} [mmol/L/h]	173	28.6	32.1	21.0	18.8	11.9	14.3	0.98	2.5	0.91	1.0	0.045
K_G, K_X [mmol/L]		3.14 $(=K_G)$			22.7 $(=K_X)$			-				
$K_{I,G}$, $K_{I,X}$ [mmol/L]		410 $(=K_{I,G})$			224 $(=K_{I,X})$			-				
$k_{E,j}$ [1/h]					1							
α_j [1/h]					0.1							
β_j [1/h]					0.2							

Finally, the cybernetic control variables, $u_{M,j}$ and $v_{M,j}$, are computed from the following the "Matching Law" and the "Proportional Law," respectively:

$$u_{M,j} = \frac{p_j}{\sum_k p_k} \text{ and } v_{M,j} = \frac{p_j}{\max_k (p_k)} \tag{9}$$

where p_j is the return-on-investment associated with the j th mode [18,19]. The carbon uptake flux is taken here as p_j,

$$p_j = f_{c,j} e_{M,j}^{rel} r_{M,j}^{kin} \tag{10}$$

where $f_{c,j}$ is the number of carbons per unit mole of substrate taken up through the j th EM. Parameter values used in model simulations are summarized in Table 1.

Fig. 3 is an illustration of the structure of the HCM designed in this article. The valves on the pathways indicate that the uptake fluxes through individual EMs are regulated such that the total (carbon) uptake flux is maximized. For simplicity, the HCM is written in an abstract form as follows:

$$\dot{\mathbf{y}} = \mathbf{g}(\mathbf{y}, \theta) \tag{11}$$

where
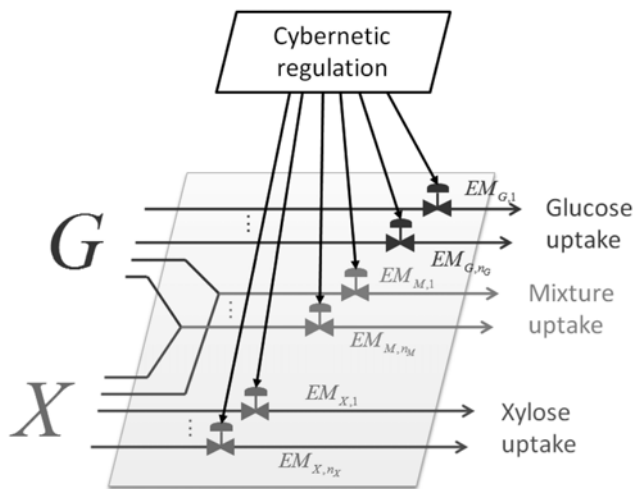
Fig. 3. Conceptual representation of hybrid cybernetic modeling: G=glucose, X=xylose, EM=elementary mode.

$$\mathbf{y} = \begin{bmatrix} \mathbf{x} \\ \mathbf{e} \end{bmatrix} \tag{12}$$

and θ is the vector of n_θ manipulated variables.

FORMULATION OF OPTIMIZATION PROBLEMS

1. Optimization Problem in Batch Reactors

The goal of optimization of batch fermentation systems is to determine optimal initial concentrations of glucose and xylose to maximize ethanol productivity. Fermentation time is also adjusted such that the total sugar conversion exceeds a certain criterion. Since the sugar level is basically given from the chosen raw materials (i.e., lignocellulosic biomass), we actually determine the extra amount of sugars to add, along with fermentation time.

The optimization problem in batch culture is formulated as follows:

$$\max_{x_{XYL,0}, t_f} P_{ETH} \tag{13}$$

such that

$$x_{GLC,0} = x_{GLC}^* \tag{14}$$

$$x_{XYL,0} \geq x_{XYL}^* \tag{15}$$

$$\xi \geq \xi^* \tag{16}$$

$$\dot{\mathbf{y}} = \mathbf{g}(\mathbf{y}, x_{GLC,0}, x_{XYL,0}) \text{ for } 0 \leq t \leq t_f \tag{17}$$

where P_{ETH} is the bioethanol productivity, $x_{GLC,0}$ and $x_{XYL,0}$ are the initial concentrations of glucose and xylose, respectively, x_{GLC}^* and x_{XYL}^* are the concentrations of glucose and xylose given from the lignocellulosic biomass, respectively, t_f is the fermentation time, ξ is the total sugar conversion, and ξ^* is the required conversion of the total sugars. Ethanol productivity and sugar conversion, respectively, are defined in batch systems as follows:

$$P_{ETH} \equiv \frac{x_{ETH,f} - x_{ETH,0}}{t_s + t_f} \tag{18}$$

$$\xi \equiv 1 - \frac{x_{GLC,f} + x_{XYL,f}}{x_{GLC,0} + x_{XYL,0}} \tag{19}$$

where x_{ETH} is the ethanol concentration, t_s is the additional time taken in batch fermentation for shutdown and startup (harvesting, clean-

ing, sterilizing, and filling), and the subscripts 0 and f denote the material concentrations at the initial and final times, respectively. The extra time taken for shutdown and startup (t_s) varies depending on the size of equipment in the range of 3 to 9 hours [20], and is assumed to be 6 hours in this work. The concentration ratio of lignocelluosic sugars (x^*_{XYL}/x^*_{GLC}) is set to be 0.5, considering the range of sugar compositions in lignocelluosic biomass [6,21], not only here in batch culture, but also in continuous culture.

The initial inoculum size (c_0) is determined to be 10% of the maximal attainable cell concentration, $c^{max}/c_0 \approx 10$, which is 10 to 20 in most commercial fermentations [20]. In this article, c^{max} is approximated using the following equation:

$$c^{max} \approx c_0 + Y_{B/GLC} x_{GLC,0} + Y_{B/XYL} x_{XYL,0} \tag{20}$$

where $Y_{B/GLC}$ and $Y_{B/XYL}$ are the biomass yields from glucose and xylose, respectively. From experimental data of Krishnan et al. [12], we determined $Y_{B/GLC}=0.165$, and $Y_{B/XYL}=0.163$.

2. Optimization Problem in Continuous Reactors

In continuous systems, we determine optimal concentrations of glucose and xylose in the feed to maximize the bioethanol productivity. The dilution rate is adjusted to meet the prescribed criterion on the total sugar conversion. The optimization problem of chemostats is formulated as follows:

$$\max_{x_{XYL,IN}, D} P_{ETH} \tag{21}$$

such that

$$x_{GLC,IN} = x^*_{GLC} \tag{22}$$

$$x_{XYL,IN} \geq x^*_{XYL} \tag{23}$$

$$\xi \geq \xi^* \tag{24}$$

$$\mathbf{0} = \mathbf{g}(\mathbf{y}, x_{GLC,IN}, x_{XYL,IN}, D) \tag{25}$$

where P_{ETH} is the bioethanol productivity, $x_{GLC,IN}$ and $x_{XYL,IN}$ are the *inlet* concentrations of glucose and xylose, respectively, and D is

the dilution rate. Ethanol productivity and sugar conversion, respectively, are defined in continuous systems as follows:

$$P_{ETH} \equiv (x_{ETH,OUT} - x_{ETH,IN})D \tag{26}$$

$$\xi \equiv 1 - \frac{x_{GLC,OUT} + x_{XYL,OUT}}{x_{GLC,IN} + x_{XYL,IN}} \tag{27}$$

where the subscript *IN* denotes the material concentrations at the inlet.

RESULTS AND DISCUSSION

1. Optimal Conditions for Batch Reactors

As described in the foregoing section, we seek the optimal values for initial xylose concentration and fermentation time in batch systems such that the bioethanol productivity is maximized under the constraint that the fractional conversion of the total sugar should be more than 0.99. Fig. 4(a) shows ethanol productivity over the space of $x_{GLC,0}$ with the range of 20 to 80 g/L, and $x_{XYL,0}/x_{GLC,0}$ with the range of 0 to 2. The highest productivity is trivially found at the corner when $x_{GLC,0}=80$ g/L and $x_{XYL,0}/x_{GLC,0}=0$ (fermentation of pure glucose). This is, however, not a reachable condition due to the constraint that $(x_{XYL,0}/x_{GLC,0}) \geq (x^*_{XYL}/x^*_{GLC})=0.5$. In Fig. 4(b), it is shown that the optimal ratio of xylose to glucose can be its lower or upper limit depending on the initial glucose concentrations. For example, when $x_{GLC,0}=20$ g/L, it is advantageous to add more xylose to the medium in order to increase productivity (i.e., from 0.47 to 0.67). The same remedy causes the exactly opposite outcome when $x_{GLC,0}=80$ g/L, i.e., addition of extra xylose worsens the productivity (from 1.4 to 1.26). Meanwhile, no appreciable improvement is observed when $x_{GLC,0}=50$ g/L.

Addition of extra xylose may have two counteracting effects on ethanol productivity. Basically, it can promote simultaneous consumption of glucose and xylose as the uptake rate of xylose is comparable to that of glucose due to the increased concentration of xylose. It is the natural tendency of cells to consume substrates which can
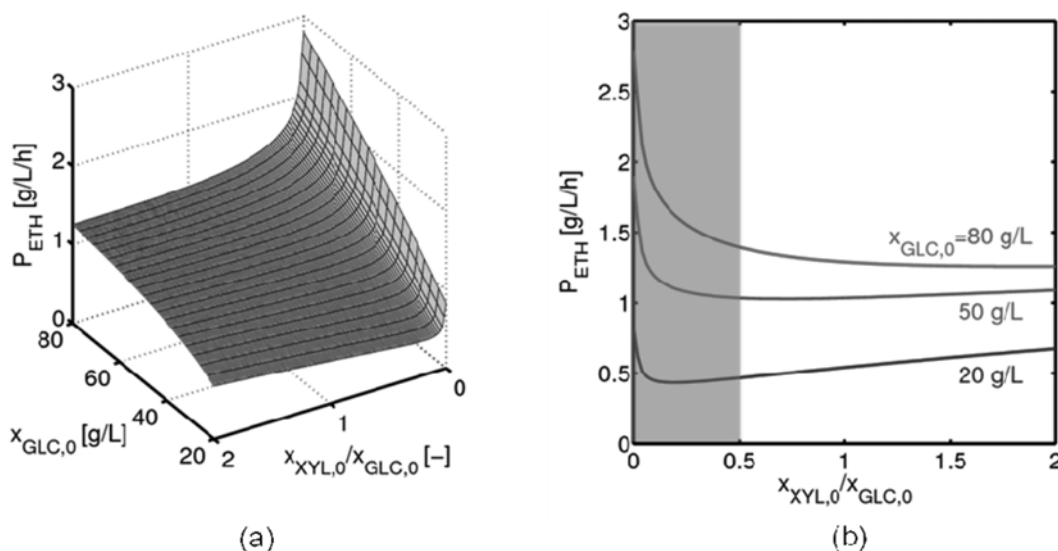

(a)

(b)

Fig. 4. Ethanol productivity with sugar concentrations in batch systems: (a) three dimensional representation, (b) two dimensional representation.
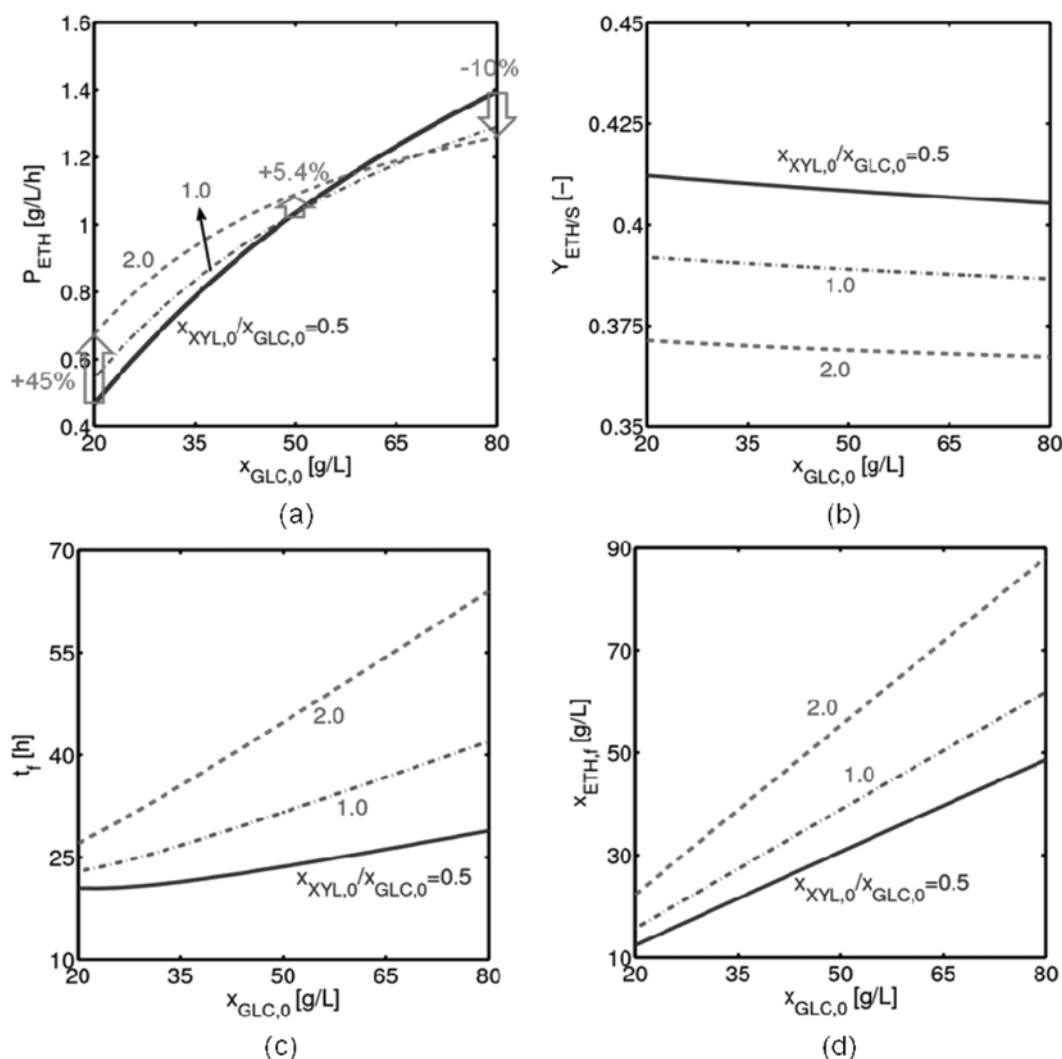
Fig. 5. Basic performance curves of batch systems: (a) ethanol productivity, (b) ethanol yield, (c) fermentation time, (d) ethanol concentration at the end time.

be more quickly metabolized. However, the increased initial concentration of xylose may prolong the fermentation time at the same time due to its low rate of metabolism. When the second effect is more dominant, the productivity gets lower as the portion of xylose increases as in the case that $x_{GLC,0}$=80 g/L. Thus, the strategy for increasing the ethanol productivity in batch fermentation should be cautiously determined considering these aspects.

Fig. 5(a) shows the change of ethanol productivity with initial glucose concentration for a given ratio of initial sugar concentrations. Ethanol productivity may or may not increase with the ratio of xylose to glucose concentration depending on initial glucose concentrations. In the case the upper limit of $x_{XYL,0}/x_{GLC,0}$ is 1.0, for example, xylose addition results in increase (or decrease) of productivity when $x_{GLC,0}$ is below (or above) about 50 g/L. If the ratio of initial sugar concentration is allowed to vary up to 2.0, such threshold is extended to $x_{GLC,0}$=58 g/L. Higher improvement of ethanol productivity is expected for lower initial concentrations of glucose (e.g., 45% up at $x_{GLC,0}$=20 g/L, but 5.4% up at $x_{GLC,0}$=50 g/L). Optimal operating conditions correspond to segments of curves above other ones. In Fig. 5(a), for example, optimal operating conditions

imply that $x_{XYL,0}/x_{GLC,0}$=2 when $20 \leq x_{GLC,0} \leq 58$, and $x_{XYL,0}/x_{GLC,0}$=0.5 when $58 \leq x_{GLC,0} \leq 80$. Fig. 5(b) to 5(d) show the change of ethanol yield from mixed sugars, fermentation time, and ethanol concentration at the end of fermentation, respectively, over the same range of $x_{GLC,0}$. These variables monotonically increase (fermentation time and ethanol concentration) or decrease (ethanol yield) with xylose addition.

Fig. 6 shows the effects of variation of operating conditions such as sugar conversion (Fig. 6(a)), initial inoculum size (Fig. 6(b)), and preculture history (Fig. 6(c)). Productivity gets higher as the sugar conversion is set lower and/or as initial inoculums size higher (Figs. 6(a) and 6(b)). Throughout simulations in this article, it is assumed that cells are precultured on xylose before entering the main culture. This assumption is reasonable in the situation that cells are recycled for the next batch since the medium contains only xylose as substrates at the end of fermentation. Higher ethanol productivity is expected when cells are pregrown on xylose, rather than glucose, because initial enzyme setting favorable for xylose fermentation is likely to promote simultaneous sugar consumption (Fig. 6(c)). Preculture effects have not been considered by general metabolic mod-
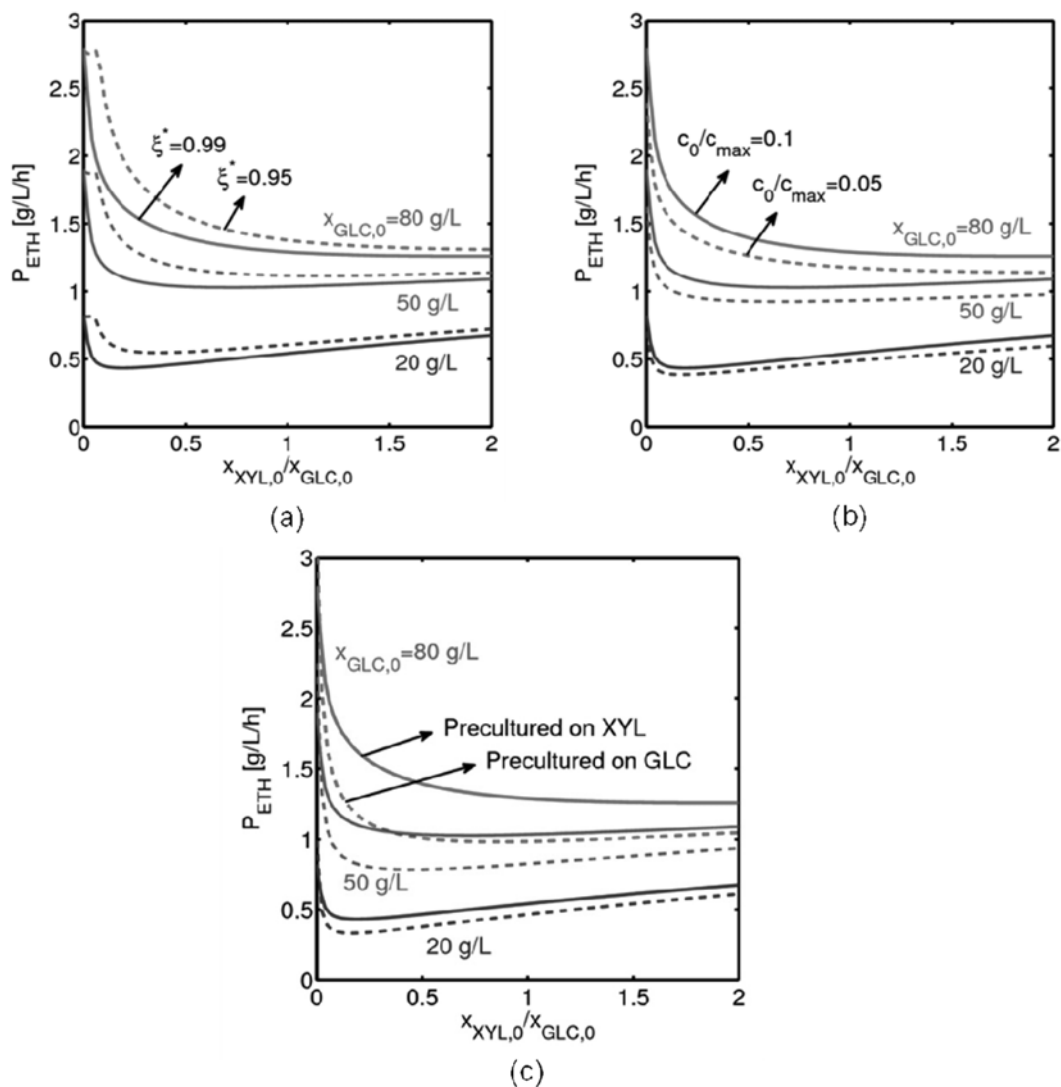
Fig. 6. Effect of (a) sugar conversion, (b) initial inoculum size, and (c) preculture history on ethanol productivity in batch systems.
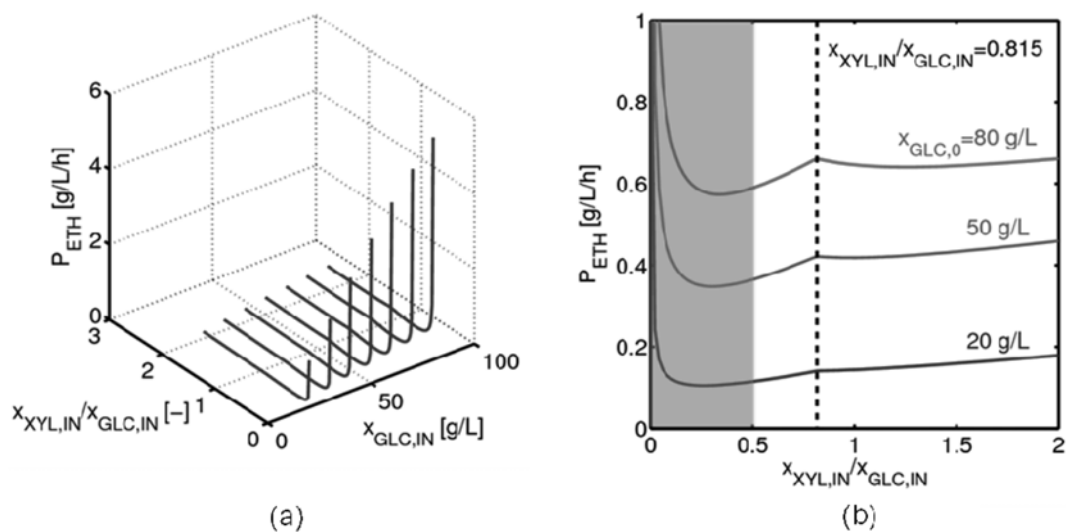

Fig. 7. Ethanol productivity with sugar concentrations in continuous systems: (a) three-dimensional representation, (b) two-dimensional representation.

eling approaches other than cybernetic models, but are readily accounted for here by setting up initial enzyme levels:

$$e_G^{rel,0}=0.091, \ e_X^{rel,0}=0.51 \ \text{(when precultured on xylose)} \quad (28)$$

and

$$e_G^{rel,0}=0.51, \ e_X^{rel,0}=0.091 \ \text{(when precultured on glucose)} \quad (29)$$

where $e_G^{rel,0}$ and $e_X^{rel,0}$ denote initial enzyme levels for glucose- and xylose-consuming EM groups. Enzyme levels for EMs consuming the mixture are determined by combination of $e_G^{rel,0}$ and $e_X^{rel,0}$ according to stoichiometry as described in Song et al. [10].

2. Optimal Conditions for Continuous Reactors

For continuous fermentation systems, we aim to determine the optimal feed composition along with dilution rate. Similar constraints are imposed as in batch fermentation, i.e., ξ^*=0.99 and ($x_{XYL,IN}$/$x_{GLC,IN}$)$\geq$(x_{XYL}^*/x_{GLC}^*)=0.5. Fig. 7 is the counterpart of Fig. 4. Several different aspects are found in continuous systems. First, addition of extra xylose to the feed is always desirable with respect to productivity enhancement. Second, multiple maxima of ethanol productivity are found at higher glucose concentrations in the feed. Third,

the critical sugar ratio at which the ethanol productivity peaks is uniquely found at around 0.815 in the present case regardless of glucose concentration.

Dependence of the ethanol productivity on $x_{GLC,IN}$ and $x_{XYL,IN}$/$x_{GLC,IN}$ is somewhat complex. In the case of $x_{GLC,IN}$=80 g/L, for example, the ethanol productivity increases as the xylose concentration in the feed increases until $x_{XYL,IN}$/$x_{GLC,IN}$ reaches 0.815, after which it drops a little bit, eventually followed by upturn (Fig. 7(b)). On the other hand, monotonic increase of ethanol productivity is observed when $x_{GLC,IN}$=20 g/L. While it is not straightforward to interpret these peculiar behaviors, it can be ascribed to interactions among the following three counteracting factors accompanied by xylose addition. That is, the first increase of ethanol productivity may be due to the promoted simultaneous consumption, the subsequent drop due to the low dilution rate which is necessary to achieve the prescribed conversion of sugars with high portion of xylose, and finally the eventual uplift due to the higher concentration of biomass as dilution rate gets lower.

Operating curves in continuous fermentation are presented in Fig. 8. Fig. 8(a) shows that, unlike the batch case, it is always recom-
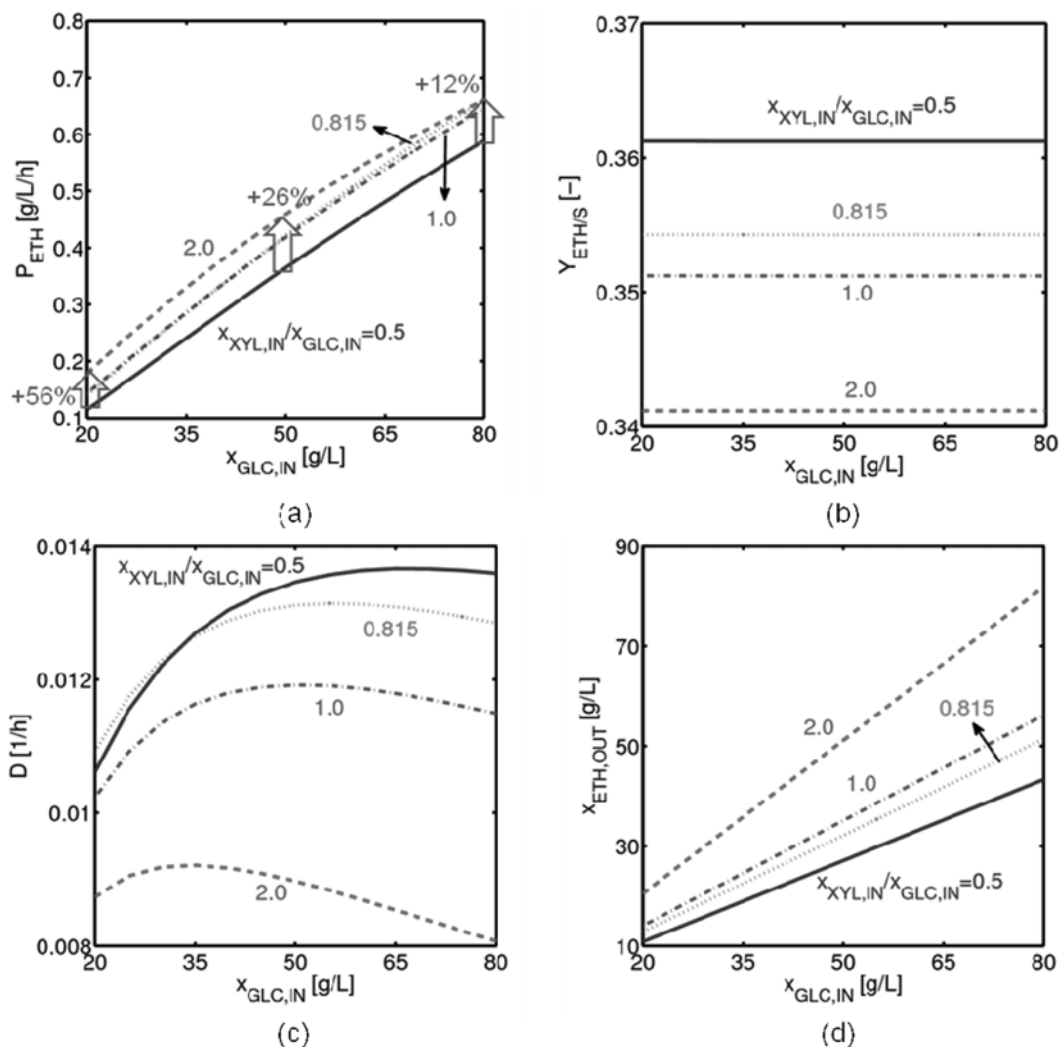

Fig. 8. Basic performance curves of continuous systems: (a) ethanol productivity, (b) ethanol yield, (c) dilution rate, (d) ethanol concentration at the outlet.
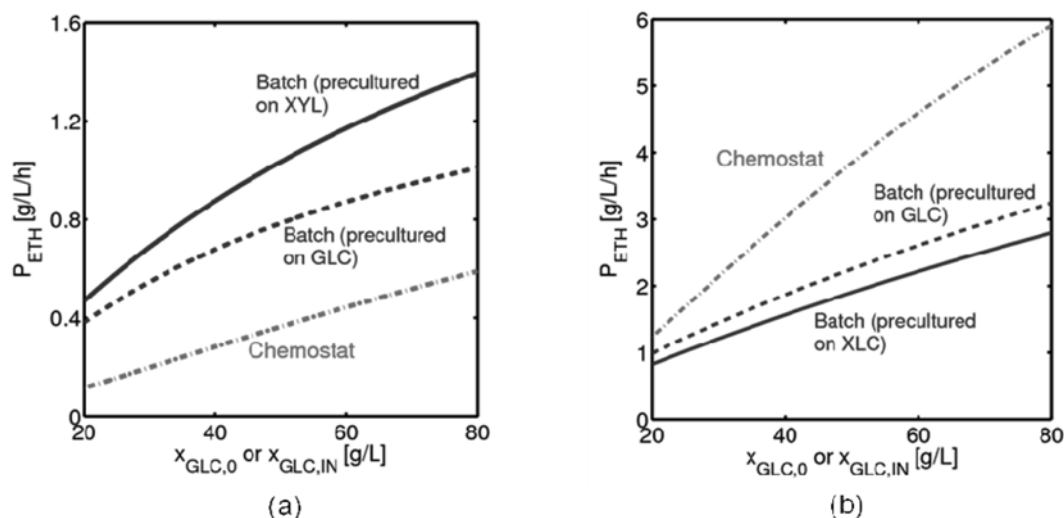
Fig. 9. Performance comparison between batch and continuous systems: (a) fermentation of mixed sugars, (b) fermentation of glucose only.

mendable to increase xylose level in the feed to increase the ethanol productivity as discussed above. The optimal sugar ratio or optimal amount of xylose to add depends on the given glucose concentration. In the range of 20 to 50 g/L of glucose, there is no difference between 0.815 and 1.0 in $x_{XYL,IN}/x_{GLC,IN}$, and after 50 g/L of glucose, $x_{XYL,IN}/x_{GLC,IN}=0.815$ leads to higher productivity that $x_{XYL,IN}/x_{GLC,IN}=$ 1.0. The best productivity is obtained when $x_{XYL,IN}/x_{GLC,IN}=2.0$, which increases the productivity by 56%, 26%, and 12% at $x_{GLC,IN}=20$, 50, and 80 g/L, respectively. Ethanol yield (Fig. 8(b)) and concentration (Fig. 8(d)) vary monotonically with the ratio of inlet sugar concentrations while dilution rate (Fig. 8(d)) is somewhat complex.

3. Comparison of Batch and Continuous Cultures

Ethanol productivity curves at standard conditions in batch and continuous systems are collected together in Fig. 9 for clear comparison. In general, the productivity of growth-associated products in a chemostat is far higher than in a batch reactor. This is not the case with ethanol production because it is suppressed by growth [20]. The ethanol productivity from mixed sugars in batch culture is about two to three times higher than in continuous culture (Fig. 9(a)). Meanwhile, the foregoing considerations show that chemostats outperform batch fermenters in ethanol production from glucose alone as cells grow relatively fast (Fig. 9(b)). Choice of preculture medium affects ethanol productivity of batch fermentation and its effect is more clearly shown for mixed sugars (Fig. 9(a)) than a single substrate (Fig. 9(b)).

At present, nearly all of the commercial production of ethanol uses batch culture. In addition to the issue of productivity, genetic instability is another reason for preference of batch culture to continuous culture [20]. Since the production of bioethanol from lignocelluosic sugars uses genetically modified yeast strains, genetic stability is a practically important issue. It is likely that the less-productive, but fast-growing yeast variants become dominant after several generations in continuous reactors while this problem might be less severe in the batch mode. On the other hand, batch fermentation has several disadvantages such as intensive labor, variability in product quality (from batch to batch), and strong inhibition by sub-

Table 2. Comparison of model estimation with experimental data

$x_{GLC,0}$ [g/L]	$x_{XYL,0}$ [g/L]	t_f [h]	ξ [-]		P_{ETH} [g/L/h]	
			Exp.	Model	Exp.	Model
114.6	0	13	0.930	0.940	2.82	2.33
0	52.12	36	0.946	0.999	0.49	0.41
56.3	52.8	24	0.863	0.836	1.48	1.35
27.7	58.6	24	0.891	0.868	1.12	1.07

strates or toxic by-products (e.g., furfural). Thus, we may need to consider various modified forms of batch and continuous reactors for commercial use, such as fed-batch operation, use of immobilized cells, and other reactor configurations [20].

4. Comparison of Model Simulations with Experimental Data

Model estimations for ethanol productivity and sugar conversion are compared with batch fermentation data available in the literature [12]. Values for productivity and conversion are calculated using Eqs. (18) and (19), respectively, from simulation curves and experimental data at specific times. Table 2 shows reasonable agreement between them, supporting the simulation results obtained in this work. Full validation on productivity increase with xylose addition of course requires additional data.

CONCLUSION

Through *in silico* analysis using a high-fidelity dynamic metabolic model including metabolic regulation, we investigate the possibility of increasing ethanol productivity of fermentation systems at the reactor level. In contrast with a general perception, higher portion of xylose relative to glucose can lead to effective elevation of ethanol productivity by promoting simultaneous sugar consumption. It is likely that actual increase of ethanol productivity obtained in reality can be less than that predicted in this theoretical work, since inhibition effect by some chemicals such as furfural other than ethanol can be practically serious but not accounted for here. Thus,

our future work includes extension of the model to incorporate this aspect, followed by experimental validation. The optimal operating curves obtained in this work provide various process alternatives for improving the productivity of bioethanol.

ACKNOWLEDGMENTS

NOMENCLATURE

Acronyms
EM : elementary mode
ETH : ethanol
GLC : glucose
XYL : xylose
MIX : mixture

Variables and Parameters
c : biomass concentration [g/L]
c_0 : initial biomass concentration [g/L]
c^{max} : theoretical maximal biomass concentration [g/L]
D : dilution rate [1/h]
e_M^{max} : maximal enzyme level
e_M^{rel} : relative enzyme level
f_c : number of carbons contained in unit mole of substrates
k_E : rate constant for inducible enzyme synthesis [1/h]
K_G : Michaelis-Menten constant for the EM group consuming glucose [mmol/L]
$K_{I,G}$: Ethanol inhibition constant for the EM group consuming glucose [mmol/L]
$K_{I,X}$: Ethanol inhibition constant for the EM group consuming xylose [mmol/L]
k^{max} : maximal rate constant for substrate consumption rate [mmol/gDW/h] or [g/gDW/h]
K_X : Michaelis-Menten constant for the EM group consuming xylose [mmol/L]
n_r : number of individual reactions
n_θ : number of manipulated parameters
n_x : number of extracellular metabolites
n_z : number of EMs
p : return-on-investment
P_{ETH} : ethanol productivity [g/L/h]
r : reaction rate [mmol/gDW/h] or [g/gDW/h]
S_x : stoichiometric coefficient matrix
t : time [h]
t_f : batch fermentation time [h]
t_s : additional time for startup and shutdown of batch systems [h]
u_M : cybernetic variable controlling enzyme synthesis
v_M : cybernetic variable controlling enzyme activity
x : vector of extracellular metabolites [mmol/L] or [g/L]
$x_{ETH,0}$: initial ethanol concentration in batch fermentation [mmol/L] or [g/L]
$x_{ETH,f}$: final ethanol concentration in batch fermentation [mmol/L] or [g/L]

x_{GLC}^* : glucose concentration of lignocellulosic sugar [mmol/L] or [g/L]
$x_{GLC,f}$: final glucose concentration in batch fermentation [mmol/L] or [g/L]
$x_{GLC,0}$: initial glucose concentration in batch fermentation [mmol/L] or [g/L]
x_{IN} : vector of extracellular metabolites in the feed of continuous fermentation [mmol/L] or [g/L]
x_{XYL}^* : xylose concentration of lignocellulosic sugar [mmol/L] or [g/L]
$x_{XYL,0}$: initial xylose concentration in batch fermentation [mmol/L] or [g/L]
$x_{XYL,f}$: final xylose concentration in batch fermentation [mmol/L] or [g/L]
y : vector of extracellular metabolites and enzyme level
$Y_{B/GLC}$: biomass yield from glucose [g/g]
$Y_{B/XYL}$: biomass yield from xylose [g/g]
Z : EM matrix

Subscripts
0 : initial time
E : enzyme
f : final time
IN : inlet
M : EM
OUT : outlet

Superscripts
kin : kinetic part
max : maximal
rel : relative

Greeks
α : constitutive enzyme synthesis rate [1/h]
β : enzyme degradation rate [1/h]
μ : growth rate [1/h]
θ : manipulated parameters
ξ : sugar conversion
ξ^* : required sugar conversion

REFERENCES

1. Annual Energy Outlook 2008 With Projections to 2030, U.S. Department of Energy, Energy Information Administration (2008).
2. S. Fetter, *The Bulletin of the Atomic Scientists*, 28 (2000).
3. W. E. Mabee, *Biofuels*, **108**, 329 (2007).
4. A. J. A. van Maris, D. A. Abbott, E. Bellissimin, J. van den Brink, M. Kuyper, M. A. H. Luttik, H. W. Wisselink, W. A. Scheffers, J. P. van Dijken and J. P. Pronk, *Antonie Van Leeuwenhoek International Journal of General and Molecular Microbiology*, **90**, 391 (2006).
5. L. O. Ingram, H. C. Aldrich, A. C. C. Borges, T. B. Causey, A. Martinez, F. Morales, A. Saleh, S. A. Underwood, L. P. Yomano, S. W. York, J. Zaldivar and S. D. Zhou, *Biotechnol. Prog.*, **15**, 855 (1999).
6. J. Lee, *J. Biotechnology*, **56**, 1 (1997).
7. B. Hahn-Hagerdal, K. Karhumaa, M. Jeppsson and M. F. Gorwa-Grauslund, *Biofuels*, **108**, 147 (2007).
8. J. P. Lange, *Biofuels Bioproducts & Biorefining-Biofpr*, **1**, 39 (2007).

9. A. Wingren, M. Galbe and G. Zacchi, *Biotechnol. Prog.*, **19**, 1109 (2003).

10. H. S. Song, J. A. Morgan and D. Ramkrishna, *Biotechnol. Bioeng.*, **103**, 984 (2009).

11. D. Ramkrishna, D. S. Kompala and G. T. Tsao, *Biotechnol. Prog.*, **3**, 121 (1987).

12. M. S. Krishnan, Y. Xia, N. W. Y. Ho and G. T. Tsao, *Fuels and Chemicals from Biomass*, **666**, 74 (1997).

13. J. I. Kim, J. D. Varner and D. Ramkrishna, *Biotechnol. Prog.*, **24**, 993 (2008).

14. S. Schuster, D. A. Fell and T. Dandekar, *Nature Biotechnology*, **18**, 326 (2000).

15. S. Schuster, C. Hilgetag, J. H. Woods and D. A. Fell, *Journal of Mathematical Biology*, **45**, 153 (2002).

16. H. S. Song and D. Ramkrishna, *Biotechnol. Bioeng.*, **102**, 554 (2009).

17. W. C. Wong, H. S. Song, J. H. Lee and D. Ramkrishna, *Control Engineering Practice*, DOI:10.1016/j.conengprac.2009.09.002 (2009).

18. D. S. Kompala, D. Ramkrishna, N. B. Jansen and G. T. Tsao, *Biotechnol. Bioeng.*, **28**, 1044 (1986).

19. J. D. Young and D. Ramkrishna, *Biotechnol. Prog.*, **23**, 83 (2007).

20. M. L. Shuler and F. Kargi, *Bioprocess engineering: Basic concepts*, Prentice Hall PTR, Upper Saddle River, NJ (2002).

21. M. Sedlak and N. W. Y. Ho, *Applied Biochemistry and Biotechnology*, **113-16**, 403 (2004).